Lattice Boltzmann study of spinodal decomposition in two dimensions

Jonathan Chin* and Peter V. Coveney†
Centre for Computational Science, Department of Chemistry, Queen Mary, University of London, Mile End Road, London E1 4NS, England

(Received 6 December 2001; published 22 July 2002)

A lattice Boltzmann model using the Shan-Chen prescription for a binary immiscible fluid is described, and the macroscopic equations obeyed by the model are derived. The model is used to quantitatively examine spinodal decomposition of a two-dimensional binary fluid. This model allows examination of the early-time period corresponding to interface formation, and shows agreement with analytical solutions of the linearized Cahn-Hilliard equation, despite the fact that the model contains no explicit free-energy functional. This regime has not, to the knowledge of the authors, been previously observed using any lattice Boltzmann method. In agreement with other models, a scaling law with the exponent 2/3 is observed for late-time domain growth. Breakdown of scaling is also observed for certain sets of simulation parameters.

DOI: 10.1103/PhysRevE.66.016303 PACS number(s): 47.20.Hw, 47.55.Kf, 05.70.Ln

I. SPINODAL DECOMPOSITION

The separation of two immiscible fluids due to spinodal decomposition is a process of significant intellectual and industrial importance. Much of the theory surrounding the process has been summarized by Bray [1] and Furukawa [2].

A two-component fluid may be described by a net fluid velocity $\mathbf{U}(\mathbf{r})$ and the densities $n^A(\mathbf{r})$ and $n^B(\mathbf{r})$ of each component, at each point $\mathbf{r}$ in the fluid. In the incompressible regime, it can be useful to work with the conserved order parameter $\phi(\mathbf{r})=n^A(\mathbf{r})-n^B(\mathbf{r})$, describing the degree of separation of the fluids. The process of phase separation can be divided into several regimes, each dominated by a different physical process. For many of these regimes, it is thought that the *dynamical scaling hypothesis* holds—that is to say, snapshots of a system at two different times will have identical morphology when each snapshot is scaled by its single characteristic length scale $L(T)$, whose time dependence is of the form $L(T)\sim T^{\alpha}$.

If it is assumed that the only parameters determining the behavior of the system are the density ρ, kinematic viscosity ν, and surface tension σ, then only one length scale $L_0=\rho\nu^2/\sigma$ and one time scale $T_0=\rho^2\nu^3/\sigma^2$ may be constructed. Lengths and times L and T measured in simulations may then be described in terms of the reduced variables $\ell=L/L_0$, and $t=T/T_0$. If dynamical scaling holds for a range of phase-separating systems, then the evolution of reduced domain size ℓ plotted against the reduced time t should collapse onto the same curve for all such systems.

A. Interface formation

During the very early stages of spinodal decomposition from a deep quench, the order parameter will be very small. Small fluctuations in the order parameter will gradually become larger, as particles of a given component gradually diffuse towards one another, and away from particles of the other component. The fluid velocity will be small, so hydrodynamics may be neglected.

If the dominant phase-separation mechanism is the diffusion of particles down the gradient of chemical potential, then a treatment with the Cahn-Hilliard equation [3] is appropriate. If it is assumed that there is a potential energy $V(\phi)$ associated with the order parameter ϕ, then the evolution of the order parameter for particles of mobility M and diffusivity κ is given by

$$\frac{\partial\phi}{\partial t}=-M\nabla^2\left[-\kappa\nabla^2\phi+\frac{\partial V}{\partial\phi}\right]. \tag{1}$$

Following the treatment given in, for example, Gunton *et al.* [4], at very early times the order parameter may be treated as a small perturbation around its initial value of zero. Taylor-expanding the derivative of potential energy to second order then gives

$$\frac{\partial\phi}{\partial t}=M\nabla^2\left(-\kappa\nabla^2+\left.\frac{\partial^2 V}{\partial\phi^2}\right|_{\phi_0}\right)\phi. \tag{2}$$

Taking the Fourier transform,

$$\frac{\partial}{\partial t}\tilde{\phi}(k,t)=-Mk^2\left(-\kappa k^2+\left.\frac{\partial^2 V}{\partial\phi^2}\right|_{\phi_0}\right)\tilde{\phi}(k,t)=\omega(k)\tilde{\phi}(k,t). \tag{3}$$

Hence, the Fourier-transformed order parameter has the form $\tilde{\phi}(k,t)=\tilde{\phi}_0(k)e^{\omega(k)t}$. The structural properties of isotropic phase-separating systems are often described by the circular or spherical average of the structure factor, defined as

$$S(\mathbf{k},t)=\left\langle\left|\frac{1}{V}\int(\phi(\mathbf{r})-\overline{\phi})e^{i\mathbf{k}\cdot\mathbf{r}}\right|^2\right\rangle. \tag{4}$$

This description is particularly useful because it may be compared directly with x ray measurements. For phase separation in this regime, the structure factor takes the form

$$S(k,t)=S_0(k)e^{2\omega(k)t}. \tag{5}$$

From Eq. (3), it can be seen that $\omega(k)$ is positive for wave vectors smaller than a critical value k_c. For such wave vec-

*Electronic address: j.chin@qmul.ac.uk
†Electronic address: p.v.coveney@qmul.ac.uk

tors, the structure factor retains the same shape, but grows exponentially in magnitude with time; the growth rate is a function $\omega(k)$ of wavelength. If there is a large peak in the structure factor, its position will stay the same while it grows, and there will be no change in the dominant length scale of the phase-separating system.

Once domains containing a majority of one particular component have formed, domain growth may proceed through the Lifshitz-Slyozov ripening mechanism, where droplets of the minority phase form and ripen through an evaporation-condensation mechanism, giving rise to a $t^{1/3}$ growth law [1].

Evidence for Lifshitz-Slyozov growth has been seen in Langevin models without hydrodynamics [5,6], dissipative particle dynamics (DPD) [7], Monte Carlo renormalization-group studies [8], and lattice Boltzmann studies [9,10].

B. Viscous hydrodynamic growth

Once sharp interfaces have formed and hydrodynamics has become important, one of several growth mechanisms may come into play.

In the viscous hydrodynamic regime, the viscous term in the Navier-Stokes equation predominates over the inertial term $\nu\nabla^2\mathbf{U}\sim 1/\rho\nabla p$, for pressure p. Assuming that dynamical scaling holds, and taking $p\sim\sigma/L$, suggests that $L\sim T$. This linear growth law was predicted by Siggia [11]; however, San Miguel *et al.* [12] showed that Siggia's growth mechanism would only occur in three dimensions, and not in two. Instead, they proposed a $t^{1/2}$ growth law based around interface diffusion.

For two-dimensional (2D) systems, early-time $t^{1/2}$ growth has been observed in molecular dynamics (MD) simulations [13,14], DPD [15,16], lattice-gas automata (LGA) [17], and a lattice Boltzmann model [18]. Other lattice Boltzmann models have produced a $t^{1/3}$ growth law [10,19], which has also been observed in models that did not conserve momentum [8,20].

C. Inertial hydrodynamic growth

If the Reynolds number of the system becomes sufficiently high, the inertial term in the Navier-Stokes equation dominates the viscous term; a brief dimensional analysis as above then suggests a $t^{2/3}$ growth law, as predicted by Furukawa [2] for times much larger than T_0. Grant and Elder [21] suggested that for very high Reynolds numbers, turbulent remixing would slow the domain coarsening process to a $t^{1/2}$ law; however, but this has not yet been observed, and it has been pointed out [15] that their assumptions are debatable.

A $t^{2/3}$ late-time growth law in two dimensions has been seen in several numerical simulations, such as Ginzburg-Landau models [20], DPD [7], and lattice Boltzmann models [19,18,22,23].

The purpose of this paper is to make a quantitative analysis of 2D spinodal decomposition using the Shan-Chen lattice Boltzmann model, comparing if, where appropriate, with behavior reported from other models.

II. WHY A LATTICE BOLTZMANN MODEL?

The lattice Boltzmann model provides a useful way of simulating hydrodynamics. It is very simple to implement, and since most lattice Boltzmann equation (LBE) models only require interactions between nearest-neighbor sites on the lattice, it scales well on massively parallel computers. It runs substantially faster than MD and LGA methods, since it neither tracks every molecule in the system as MD does, nor requires as much ensemble averaging as LGA. In addition, it is easily modified to incorporate an arbitrary number of interacting fluid components.

Lattice Boltzmann studies of spinodal decomposition have already been done in two [19] and three [24] dimensions, producing interactions between the components either by forcing immiscibility in a manner similar to the Rothman-Keller method for LGA models [25,26], or by positing a macroscopic free-energy functional that must be minimized. The latter approach has the advantage that macroscopic parameters such as surface tension may be chosen and supplied directly to the model. However, such a ''top-down'' approach gives little information about how the microscopic interactions in a system give rise to its macroscopic behavior, and it is not always clear that such a free-energy approach is valid in systems that are far from equilibrium.

The ''bottom-up'' Shan-Chen model described below takes a different approach by specifying an explicit interaction force between components, which drives the phase separation. Phase separation has been examined qualitatively [27] using the Shan-Chen model, but until now no quantitative studies have been made. The results of the studies presented here suggest that phenomena very similar to those examined with free-energy models, including the very early stage of interface formation, may be studied using the Shan-Chen approach.

III. 2D LATTICE BOLTZMANN MODEL FOR IMMISCIBLE FLUIDS

Lattice Boltzmann models describe the evolution of a single-particle distribution function f_i^σ defined on a discrete lattice of points $\mathbf{x}$, where each point is connected to its ith nearest neighbor by a vector $\mathbf{c}_i$. $f_i^\sigma(\mathbf{x},t)$ is proportional to the number of particles of component σ at site $\mathbf{x}$ at time t traveling with velocity $\mathbf{c}_i$, so that the number density n^σ and velocity $\mathbf{u}^\sigma$ of component σ are given by

$$n^\sigma(\mathbf{x})=\sum_i f_i^\sigma(\mathbf{x}), \tag{6}$$

$$n^\sigma\mathbf{u}^\sigma(\mathbf{x})=\sum_i f_i^\sigma(\mathbf{x})\mathbf{c}_i. \tag{7}$$

Many lattice Boltzmann models use the ''lattice Bhatnagar-Gross-Krook (BGK)'' ansatz, where, after a streaming step where particles move to adjacent sites, the distribution function relaxes to an equilibrium value $N_i(n^\sigma,\mathbf{U})$, chosen to be some function of the macroscopic fluid velocity $\mathbf{U}$ that produces the correct hydrodynamic behavior:

$$f_i^\sigma(\mathbf{x}+\mathbf{c}_i,t+1)-f_i^\sigma(\mathbf{x},t)=-\frac{1}{\tau^\sigma}[f_i^\sigma(\mathbf{x},t)-N_i(n^\sigma,\mathbf{U})]. \tag{8}$$

Shan and Chen [28] introduced a modification to this model to allow the simulation of fluids with many interacting components. The equilibrium value of the distribution function for a given component is now set to be a function not of the total fluid velocity $\mathbf{U}$ at a site, but of a velocity $\mathbf{v}^\sigma$, where

$$\mathbf{v}^\sigma=\mathbf{u}'+\frac{\tau^\sigma}{\rho^\sigma}\mathbf{F}^\sigma, \tag{9}$$

$$\mathbf{u}'=\left(\sum_\sigma \frac{\rho^\sigma}{\tau^\sigma}\mathbf{u}^\sigma\right)\Big/\left(\sum_\sigma \frac{\rho^\sigma}{\tau^\sigma}\right). \tag{10}$$

Here, $\rho^\sigma=m^\sigma n^\sigma$ is the mass density of component σ, and $\mathbf{F}^\sigma$ is the force acting on that component. The form of the interaction force was given in terms of an arbitrary function $\psi^\sigma(\mathbf{x})=\psi[n^\sigma(\mathbf{x})]$ of the density of each component at each site:

$$\mathbf{F}^\sigma=-\psi^\sigma(\mathbf{x})\sum_{\bar{\sigma}} g_{\sigma\bar{\sigma}}\sum_i \psi^{\bar{\sigma}}(\mathbf{x}+\mathbf{c}_i)\mathbf{c}_i. \tag{11}$$

The interaction strength between components σ and $\bar{\sigma}$ is controlled by the coupling constant $g_{\sigma\bar{\sigma}}$.

Many lattice Boltzmann models, including the original Shan-Chen model, have been performed on lattices on which the lattice tensors $T^{(n)}_{\alpha_1\ldots\alpha_n}=\Sigma_i c_{i\alpha_1}\cdots c_{i\alpha_n}$ are isotropic up to fourth order, so that isotropic hydrodynamics can be recovered. The only regular lattice in 2D with the appropriate properties is the hexagonal ''FHP'' lattice [29,30], although a hydrodynamic lattice-gas model has recently been constructed on a simpler irregular lattice [31]. Qian *et al.* [32] pointed out that the correct hydrodynamic behavior can be recovered from certain anisotropic regular lattices, provided that a modified equilibrium distribution is used, incorporating a weighting factor T_i for each lattice vector $\mathbf{c}_i$:

$$N_i(n,\mathbf{U})=nT_i\left[1+\frac{c_{i\alpha}U_\alpha}{c_s^2}+\frac{U_\alpha U_\beta}{2c_s^2}\left(\frac{c_{i\alpha}c_{i\beta}}{c_s^2}-\delta_{\alpha\beta}\right)\right]. \tag{12}$$

The weighting factors are chosen such that the tensors $T^{(n)}_{\alpha_1\ldots\alpha_n}=\Sigma_i T_i c_{i\alpha_1}\cdots c_{i\alpha_n}$ are isotropic to fourth order, that is to say,

$$T^{(1)}_\alpha=0, \tag{13}$$

$$T^{(2)}_{\alpha\beta}=c_s^2\delta_{\alpha\beta}, \tag{14}$$

$$T^{(3)}_{\alpha\beta\gamma}=0, \tag{15}$$

$$T^{(4)}_{\alpha\beta\gamma\delta}=c_s^4(\delta_{\alpha\beta}\delta_{\gamma\delta}+\delta_{\alpha\delta}\delta_{\beta\gamma}+\delta_{\alpha\gamma}\delta_{\beta\delta}). \tag{16}$$

It can be shown [33] that the constant c_s^2 is the squared speed of sound of the model. Some straightforward algebra shows that $n=\Sigma_i N_i(n,\mathbf{U})$ and $\mathbf{U}=\Sigma_i N_i(n,\mathbf{U})\mathbf{c}_i$.

In order to use the Shan-Chen interaction system for models on such anisotropic lattices, a weighting factor must be included in the force term, modifying Eq. (11) to give

$$\mathbf{F}^\sigma=-\psi^\sigma(\mathbf{x})\sum_{\bar{\sigma}} g_{\sigma\bar{\sigma}}\sum_i T_i\psi^{\bar{\sigma}}(\mathbf{x}+\mathbf{c}_i)\mathbf{c}_i. \tag{17}$$

This may be written as a Taylor expansion:

$$\psi^{\bar{\sigma}}(\mathbf{x}+\mathbf{c}_i)\simeq\psi^{\bar{\sigma}}(\mathbf{x})+c_{i\beta}\partial_\beta\psi^{\bar{\sigma}}(\mathbf{x})+\tfrac{1}{2}c_{i\beta}c_{i\gamma}\partial_\beta\partial_\gamma\psi^{\bar{\sigma}}(\mathbf{x})+\cdots. \tag{18}$$

Substituting this expansion into Eq. (17) and using the isotropy property of the lattice tensors to simplify, gives, to third order,

$$\mathbf{F}=\sum_\sigma \mathbf{F}^\sigma\simeq-c_s^2\nabla\left(\sum_{\sigma\bar{\sigma}}\psi^\sigma g_{\sigma\bar{\sigma}}\psi^{\bar{\sigma}}\right). \tag{19}$$

c_s^2 is the speed of sound, which may be derived from the lattice properties.

In the Shan-Chen model, the momentum at a site is changed during both the advection step and the collision step—momentum is not conserved locally. Because of this, the macroscopic fluid velocity must include contributions from this momentum flux. It can be shown [34,35] that defining the macroscopic velocity as the velocity at the temporal midpoint between collision and advection, or requiring that it go to zero at equilibrium, produces the same expression:

$$\rho U_\alpha=\sum_\sigma m^\sigma\sum_i f_i^\sigma c_{i\alpha}+\frac{1}{2}\sum_\sigma F_\alpha^\sigma. \tag{20}$$

Similarly, the momentum flux tensor becomes

$$\Pi_{\alpha\beta}=\sum_\sigma m^\sigma\sum_i f_i^\sigma c_{i\alpha}c_{i\beta}+\frac{1}{2}\sum_{\sigma\bar{\sigma}} g_{\sigma\bar{\sigma}}T_i\psi^\sigma(\mathbf{x})\psi^{\bar{\sigma}}(\mathbf{x}+\mathbf{c}_i)c_{i\alpha}c_{i\beta}. \tag{21}$$

It should be noted that the Shan-Chen scheme conserves the mass of each component, and the rate of change of total momentum is proportional to the force:

$$m^\sigma\sum_i \Omega_i^\sigma=0, \tag{22}$$

$$\sum_\sigma m^\sigma\sum_i \Omega_i^\sigma c_{i\alpha}=\sum_\sigma F_\alpha^\sigma. \tag{23}$$

A full derivation of a more general form of the macroscopic equations of the Shan-Chen model is presented in the Appendix.

IV. LONG-TERM STABILITY

Kendon *et al.* observed instabilities with a free-energy lattice Boltzmann model [36], and suggested that any simulation using the algorithm would eventually become unstable. The Shan-Chen model used here has certainly shown instabilities, for example, for systems with very high surface tensions, which lead to large particle velocities and numerical overflow. *Unconditional* instability has not been observed: systems that became unstable usually did so within the first few thousand time steps. As a further check on stability, a phase-separation simulation was performed on a 256×256 lattice for 2×10^6 time steps without showing any signs of instability. Between time step 1.95×10^6 and time step 2×10^6, the value in lattice units of the order parameter at any lattice site differed at most by 4.8×10^{-12}.

V. SURFACE TENSION

In order to conduct investigations of spinodal decomposition, the surface tension σ must be determined. A convenient method for doing this is to evaluate the integral of the difference between the components of the pressure tensor [as defined in Eq. (21)] perpendicular and parallel to the interface:

$$\sigma=\int_{-\infty}^{\infty}[\Pi_{\perp}-\Pi_{\parallel}]\mathrm{d}z=\int_{-\infty}^{\infty}[\Pi_{xx}-\Pi_{yy}]\mathrm{d}x. \qquad (24)$$

All simulations described here used relaxation times of $\tau^r=\tau^b=1.0$, and a mean density of 1.0. For each value of the coupling constant $g=g_{rb}=g_{br}$ [Eq. (11)] used in a phase-separation simulation, the corresponding surface tension was determined by initializing a simulation on a 128×32 grid (initially split into two 64×32 regions containing one single component), and allowing the interface to relax. The surface tension was then calculated once fluctuations had died down, usually after approximately 40 000 time steps.

VI. SPINODAL DECOMPOSITION STUDY

Spinodal decomposition simulations were performed on a 256×256 lattice. The simulations were initialized to contain a number density of $0.5+\delta$ red particles and $0.5-\delta$ blue particles at each site, where δ is randomly chosen from a uniform distribution in the range $-0.025\leqslant\delta\leqslant0.025$ at each lattice site, to provide a small initial perturbation in the order parameter. Since there are no thermal fluctuations in this lattice Boltzmann algorithm, the system would sit in a metastable state forever if both the order parameter and density were exactly uniform across the system.

A conventional measurement of the typical domain size $R(t)$ in simulations of phase separation is the inverse first moment of the circularly averaged structure factor [Eq. (4)]:

$$R(t)=2\pi\left(\sum_k S(k)\right)\Big/\left(\sum_k kS(k)\right). \qquad (25)$$

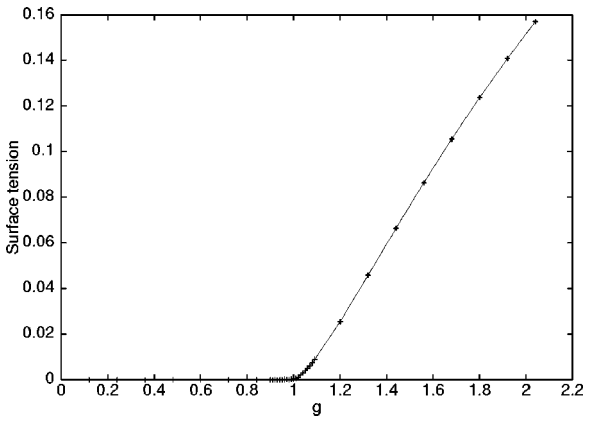

FIG. 1. Surface tension in lattice units vs coupling constant g for $\rho=1.0$ and $\tau=1.0$.

In regimes where only one length scale exists, $R(t)$ should scale with the same exponent as any other measure of domain size.

A. Interface formation

A simulation was performed with the coupling constant $g=1.08$, giving a surface tension $\sigma=0.005$, as seen in Fig. 1. For the period approximately between time steps 1000 and 5000, no change in the typical domain size $R(t)$ was observed, as can be seen in Fig. 2. However, when the structure factor $S(k)$ is plotted as a function of a wave vector, the exponential growth predicted by a Cahn-Hilliard treatment can be clearly seen, as in Fig. 3.

The wavelength-dependent growth rate $\omega(k)$ was determined from the results by fitting a straight line through a graph of $\log S(k,t)$ against t for each wave vector k. The form of $\omega(k)$ obtained is close to the quartic functional form suggested in Eq. (3), as can be seen in Fig. 4.

In Fig. 5, it can be seen that during this stage of phase separation, the sizes and positions of the domains remain roughly the same, while the interfaces between each domain gradually sharpen as separation proceeds. Once sharp interfaces have formed, the domains then begin to coarsen

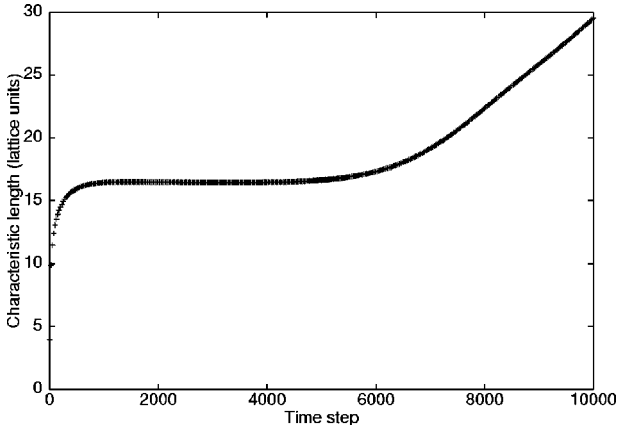

FIG. 2. Characteristic length $R(t)$ vs simulation time step, both in lattice units, for $g=1.08$, $\rho=1.0$, $\tau=1.0$.

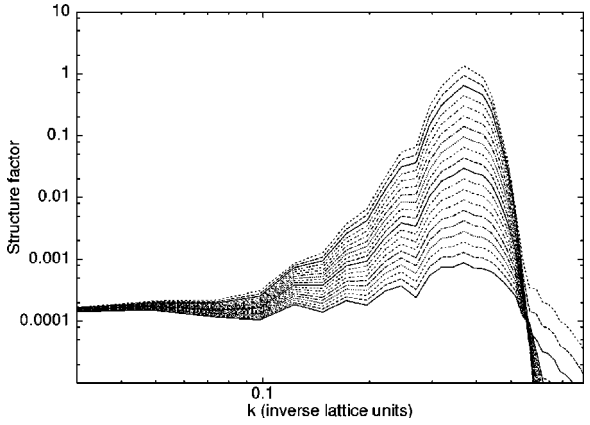

FIG. 3. The structure factor $S(k)$ plotted against wave vector k for time step 1000 (lowest curve), every 500 time steps up to time step 10 500 (highest curve). Since the vertical axis is logarithmic, the even spacing of the curves demonstrates the exponential growth present at early stages of phase separation.

through other mechanisms; the exponential growth in structure factor stops and the structure factor peak moves towards longer wavelengths.

In addition to the previously detailed analytical treatment, early-time exponential growth of the structure factor has been simulated in DPD studies [37]. Our results show that it is now also possible to examine the regime with lattice Boltzmann models. It is perhaps worth noting that the results of a free-energy Cahn-Hilliard model are reproduced here by a model that does not employ an explicit free-energy functional in its implementation of interactions between species.

B. Long-time growth exponent

Simulations were performed for parameters corresponding to reduced times $0.01 \leqslant T/T_0 \leqslant 1000$, with $T_{\max} = 10\,000$. The characteristic domain size $R(t)$ was calculated from the inverse first moment of the structure factor. The reduced domain size $R(t)/R_0$ for any simulation was observed to collapse onto the same curve, as can be seen in Fig. 6. During

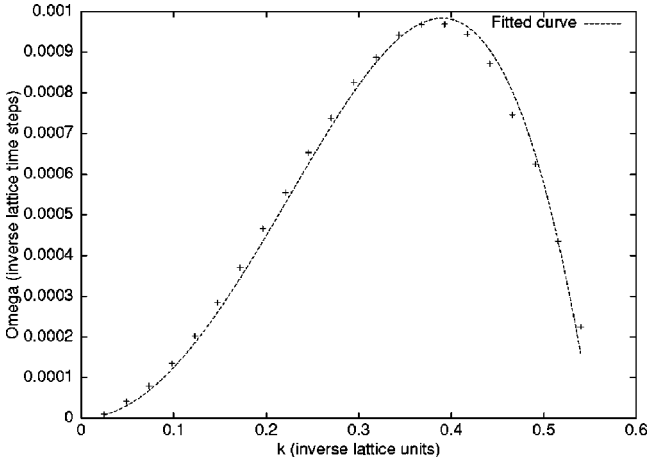

FIG. 4. Growth rate $\omega(k)$ against wave vector k compared with the analytical Cahn-Hilliard form.

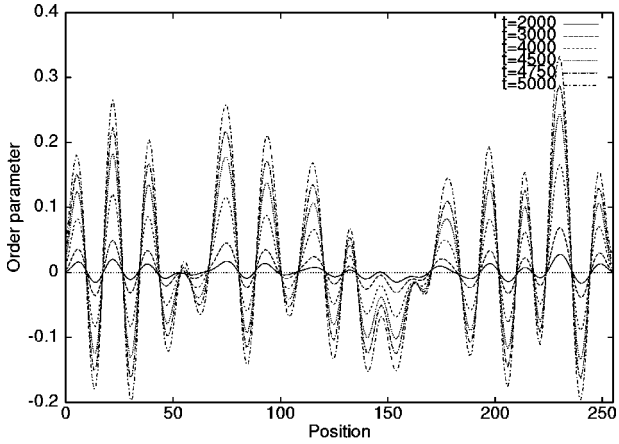

FIG. 5. A one-dimensional cross section of the lattice, showing the order parameter in lattice units vs position in lattice units, for several different time steps during the interface formation stage. Note that the domain width remains constant, while the depth increases.

the early-time period, no viscous hydrodynamic growth has been observed, since the Cahn-Hilliard mechanism appears to dominate. For large times $T \gg T_0$, the $t^{2/3}$ inertial growth law was observed. Note that since the power-law curve is of the form $R=(T-T_i)^n$ rather than T^n (T_i corresponding to the time at which interfaces have formed) the $t^{2/3}$ regime is not quite a straight line, as it would be were $T_i=0$.

If dynamical scaling holds in the $t^{2/3}$ regime, then the rescaled structure factor $F(x)=S(k,t)/R(t)^2$ of any simulation at any point in time should always have the same form when plotted against $x=kR(t)$. This can be seen in Fig. 7. According to Porod's law [8], a system with a sufficiently large amount of interface should produce a structure factor of the form $F(x) \propto x^{-3}$ for sufficiently large x in two dimensions; this curve is plotted for comparison. However, for very large wave vectors, Porod's law is not expected to be obeyed, since the corresponding length scale is similar to that of the interface width.

VII. BREAKDOWN OF SCALING

The dynamical scaling hypothesis does not always hold during phase separation, as has been observed both experi-

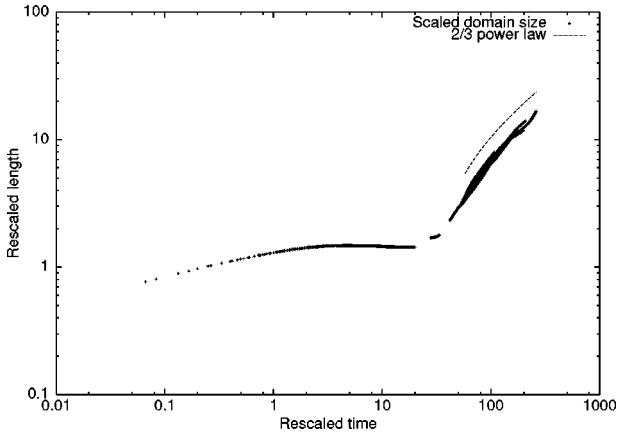

FIG. 6. Reduced domain size plotted against reduced time.

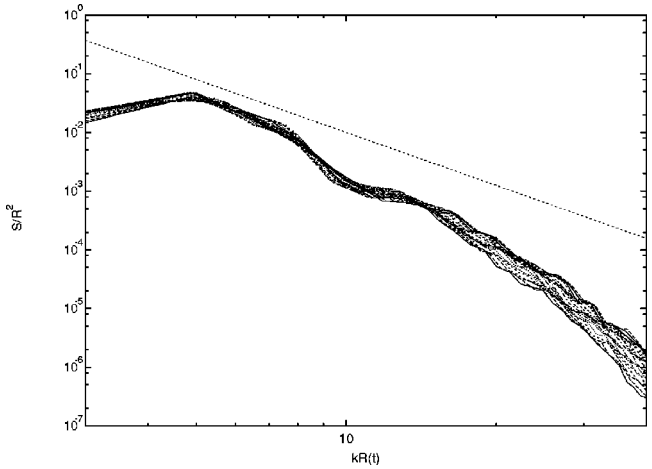

FIG. 7. Rescaled structure factor in the scaling regime, with the dotted line representing an x^{-3} curve for comparison with Porod's law.

mentally by Tanaka [38], and in free-energy lattice Boltzmann simulations by Wagner and Yeomans [9]. They all observed a regime where domains form due to hydrodynamic effects, but too quickly for the order parameter to obtain its equilibrium value, leading to a second phase separation inside the initially established domains.

The same effect has been observed with this model, for example, with the parameter set $\tau=1.8765$, $\rho=1.0$, $g=3.266$. The system quickly separates into domains, with smaller circular domains appearing at longer times, leading to a variety of length scales, as shown in Fig. 8. There is no clear scaling behavior when this effect occurs.

VIII. CONCLUSIONS

A 2D lattice Boltzmann model has been described. When used to examine spinodal decomposition, the model showed agreement with the Cahn-Hilliard theory during interface formation at very early times. Dynamical scaling was seen for the late-time inertial stage of phase separation, with the typical domain size scaling as the time raised to the power of 2/3. However, under certain circumstances, breakdown of dynamical scaling was also seen, as has been observed both experimentally and in another LBE model. Viscous-regime dynamical scaling was not observed.

For certain parameter sets, the model was found to remain numerically stable for many time steps, in contrast to a free-energy model, which apparently does not display such behavior [36]. In our model, instabilities only appear to set in for extreme values of the simulation parameters.

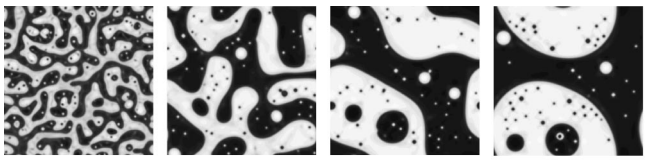

FIG. 8. Order parameter during breakdown of scaling on a 256×256 lattice. Note the many different droplet sizes at late times.

In the Appendix, we report a derivation via a Chapman-Enskog procedure of the general macroscopic equations obeyed by the model when implemented on any of the lattices described by Qian *et al.* [32]. Since the model allows for many lattice types and an arbitrary number of interacting fluid components, it should be useful for treating other complex fluids, such as those involving surfactants [39].

ACKNOWLEDGMENTS

The authors thank Queen Mary, University of London and Huntsman Polyurethanes for financial support of this work. We are grateful to Peter Love, Nélido González-Segredo, and, in particular, to Yue-Hong Qian for useful discussions.

APPENDIX: MACROSCOPIC EQUATIONS FROM THE SHAN-CHEN MODEL

The treatment below works for arbitrary numbers of immiscible or forced components, and is valid for *any* of the lattices defined by Qian *et al.* [32]. Previous Chapman-Enskog procedures for the Shan-Chen model seem to have been limited to specific lattices such as FHP, and produced macroscopic equations containing lattice-specific terms such as the number of nearest neighbors in single-velocity lattices. However, these may be absorbed into the speed of sound c_s^2, which in turn can be derived from the properties of the lattice.

1. Moments of the equilibrium distribution

By multiplying N_i^σ by the appropriate number of lattice vectors $\mathbf{c}_i$, summing over i, and substituting the relations (13–16), the following moments of the equilibrium distribution can be found:

$$m^\sigma \sum_i N_i^\sigma(\mathbf{u}) = \rho^\sigma, \tag{A1}$$

$$m^\sigma \sum_i N_i^\sigma(\mathbf{u}) c_{i\alpha} = \rho^\sigma u_\alpha, \tag{A2}$$

$$m^\sigma \sum_i N_i^\sigma(\mathbf{u}) c_{i\alpha} c_{i\beta} = \rho^\sigma (c_s^2 \delta_{\alpha\beta} + u_\alpha u_\beta), \tag{A3}$$

$$m^\sigma \sum_i N_i^\sigma(\mathbf{u}) c_{i\alpha} c_{i\beta} c_{i\gamma} = \rho^\sigma c_s^2 (u_\alpha \delta_{\beta\gamma} + u_\beta \delta_{\alpha\gamma} + u_\gamma \delta_{\alpha\beta}). \tag{A4}$$

2. Power series expansion

The collision operator may be written as a Taylor expansion in time and space:

$$\Omega_i^\sigma = f_i^\sigma(\mathbf{r}+\mathbf{c}_i, t+1) - f_i^\sigma(\mathbf{r},t) = (c_{i\alpha}\partial_\alpha + \partial_t) f_i^\sigma + \tfrac{1}{2}(c_{i\alpha}\partial_\alpha + \partial_t)(c_{i\beta}\partial_\beta + \partial_t) f_i^\sigma + \cdots.$$

The distribution function is written as a power series expansion in a parameter ϵ, used to keep terms of the same order together. This parameter will be dropped from the remainder of this treatment:

$$f_i^\sigma = f_i^{\sigma(0)} + \epsilon f_i^{\sigma(1)} + \epsilon^2 f_i^{\sigma(2)} + \cdots. \tag{A5}$$

The time derivative is also written as a series expansion, with each term corresponding to a different physical time scale. Spatial derivatives are treated as first order:

$$\partial_t = \partial_{1t} + \partial_{2t} + \cdots. \tag{A6}$$

Substituting these expansions into the Taylor series for the collision operator gives

$$\begin{aligned}\Omega_i^\sigma = {} & (c_{i\alpha}\partial_\alpha + \partial_{1t}) f_i^{\sigma(0)} + (c_{i\beta}\partial_\beta + \partial_{1t}) f_i^{\sigma(1)} \\ & + [\partial_{2t} + \tfrac{1}{2} c_{i\alpha}\partial_\alpha (c_{i\beta}\partial_\beta + \partial_{1t}) \\ & + \tfrac{1}{2}(c_{i\alpha}\partial_\alpha + \partial_{1t})] f_i^\sigma + \cdots.\end{aligned}$$

Hence, $\Omega_i^\sigma = \Omega_i^{\sigma(1)} + \Omega_i^{\sigma(2)} + \cdots$, where

$$\Omega_i^{\sigma(1)} = (c_{i\alpha}\partial_\alpha + \partial_{1t}) f_i^{\sigma(0)}, \tag{A7}$$

$$\begin{aligned}\Omega_i^{\sigma(2)} = {} & (c_{i\beta}\partial_\beta + \partial_{1t}) f_i^{\sigma(1)} + [\partial_{2t} + \tfrac{1}{2} c_{i\alpha}\partial_\alpha (c_{i\beta}\partial_\beta + \partial_{1t}) \\ & + \tfrac{1}{2}(c_{i\alpha}\partial_\alpha + \partial_{1t})] f_i^{\sigma(0)}.\end{aligned} \tag{A8}$$

In order to produce a set of macroscopic equations, the leading-order distribution function is set to be the equilibrium distribution about the macroscopic fluid velocity defined in Eq. (20), i.e.,

$$f_i^{\sigma(0)} = N_i(n^\sigma, \mathbf{U}). \tag{A9}$$

Substituting $\mathbf{U}$ into the moments (A1,A2) of the equilibrium distribution function shows that the density and macroscopic momentum may be found from the first-order equilibrium distribution function:

$$m^\sigma \sum_i f_i^{\sigma(0)} = \rho^\sigma, \tag{A10}$$

$$\sum_\sigma m^\sigma \sum_i f_i^{\sigma(0)} c_{i\alpha} = \rho U_\alpha. \tag{A11}$$

However, the full distribution function (A5) must still produce the single-component density $m^\sigma \Sigma_i f_i^\sigma$ and the kinetic momentum $m^\sigma \Sigma_i f_i^\sigma \mathbf{c}_i$. This requirement leads to restrictions on the higher-order terms in the expansion:

$$m^\sigma \sum_i f_i^{\sigma(n)} = 0 \quad \text{for} \quad n > 0, \tag{A12}$$

$$\sum_\sigma m^\sigma \sum_i f_i^{\sigma(1)} c_{i\alpha} = -\frac{1}{2} \sum_\sigma F_\alpha^\sigma, \tag{A13}$$

$$\sum_\sigma m^\sigma \sum_i f_i^{\sigma(n)} c_{i\alpha} = 0 \quad \text{for} \quad n > 1. \tag{A14}$$

For notational convenience, define the nth-order momentum flux tensors:

$$\Pi^{\sigma(\mathrm{n})}_{\alpha_1 \cdots \alpha_n} = m^\sigma \sum_i f_i^{\sigma(n)} c_{i\alpha_1} \cdots c_{i\alpha_n},$$

$$\Pi^\sigma_{\alpha_1 \cdots \alpha_n} = \Pi^{\sigma(0)}_{\alpha_1 \cdots \alpha_n},$$

$$\Pi_{\alpha_1 \cdots \alpha_n} = \sum_\sigma \Pi^\sigma_{\alpha_1 \cdots \alpha_n}.$$

Substituting the first-order expansion (A7) into the conservation relations (22,23) gives

$$\partial_\alpha \Pi_\alpha^\sigma + \partial_{1t} \rho^\sigma = 0, \tag{A15}$$

$$\partial_\beta \Pi_{\alpha\beta} + \partial_{1t} \Pi_\alpha = \sum_\sigma F_\alpha^\sigma. \tag{A16}$$

Equation (A15) describes the conservation of mass for a single component. Equation (A16) is an inviscid Euler equation for the fluid mixture, with a scalar, velocity-independent pressure proportional to the density:

$$\partial_\alpha c_s^2 \rho + \partial_\beta \rho u_\alpha u_\beta + \partial_{1t} \rho u_\alpha = \sum_\sigma F_\alpha^\sigma. \tag{A17}$$

Requiring continuity to second order gives

$$\partial_\alpha \Pi_\alpha^{\sigma(1)} + \partial_{2t} \rho^\sigma + \tfrac{1}{2} \partial_\alpha \partial_\beta \Pi_{\alpha\beta}^\sigma + \partial_{1t} \partial_\alpha \Pi_\alpha^\sigma + \tfrac{1}{2} \partial_{1t}^2 \rho^\sigma = 0. \tag{A18}$$

Equation (A15) can be differentiated to give $\partial_{1t}\partial_\alpha \Pi_\alpha^\sigma = -\partial_{1t}^2 \rho^\sigma$; substituting into (A18) gives

$$\partial_{2t} \rho^\sigma = -\partial_\alpha \Pi_\alpha^{\sigma(1)} - \tfrac{1}{2} \partial_\alpha \partial_\beta \Pi_{\alpha\beta}^\sigma + \tfrac{1}{2} \partial_{1t}^2 \rho^\sigma. \tag{A19}$$

Summing over σ, then substituting Eq. (A13) to get rid of the term in $\Pi_\alpha^{\sigma(1)}$, gives

$$\partial_{2t} \rho = \tfrac{1}{2} \partial_\alpha \sum_\sigma F_\alpha^\sigma - \tfrac{1}{2} \partial_\alpha \partial_\beta \Pi_{\alpha\beta} + \tfrac{1}{2} \partial_{1t}^2 \rho. \tag{A20}$$

The terms on the right-hand side now cancel out upon substitution of Eqs. (A15) and (A16), giving

$$\partial_{2t} \rho = 0. \tag{A21}$$

To second order, conservation of momentum gives

$$\begin{aligned}\partial_\beta \Pi_{\alpha\beta}^{\sigma(1)} + \partial_{1t} \Pi_\alpha^{\sigma(1)} + \partial_{2t} \Pi_\alpha^\sigma + \tfrac{1}{2} \partial_\beta \partial_\gamma \Pi_{\alpha\beta\gamma}^\sigma + \partial_{1t} \partial_\beta \Pi_{\alpha\beta}^\sigma \\ + \tfrac{1}{2} \partial_{1t}^2 \Pi_\alpha^\sigma = 0.\end{aligned} \tag{A22}$$

The first-order terms may be simplified by substituting the first-order terms in the BGK operator:

$$f_i^{\sigma(1)} = -\tau^\sigma (c_{i\gamma}\partial_\gamma + \partial_{1t}) f_i^{\sigma(0)}. \tag{A23}$$

This gives

$$\Pi_{\alpha}^{\sigma(1)} = -\tau^{\sigma}\partial_{\beta}\Pi_{\alpha\beta}^{\sigma} - \tau^{\sigma}\partial_{1t}\Pi_{\alpha}^{\sigma} \tag{A24}$$

$$\Pi_{\alpha\beta}^{\sigma}{}^{(1)} = \tau^{\sigma}[\partial_{\gamma}\Pi_{\alpha\beta\gamma}^{\sigma} + \partial_{1t}\Pi_{\alpha\beta}^{\sigma}]. \tag{A25}$$

Substituting into the momentum equation (A22) gives

$$\partial_{2t}\Pi_{\alpha}^{\sigma} = (\tau^{\sigma} - \tfrac{1}{2})\partial_{\beta}\partial_{\gamma}\Pi_{\alpha\beta\gamma}^{\sigma} + (\tau^{\sigma} - \tfrac{1}{2})\partial_{1t}^{2}\Pi_{\alpha}^{\sigma} + (2\tau^{\sigma} - 1)\partial_{1t}\partial_{\beta}\Pi_{\alpha\beta}^{\sigma}. \tag{A26}$$

Following, for example, Wolfram [29], the last two terms are dropped since they become negligible for a sufficiently small Mach number. This is not an entirely satisfactory move—Qian and Orszag [40] pointed out that these two terms give rise to a term cubic in the velocity, whose magnitude relative to the other terms varies roughly as the square of the Mach number. Suggestions [41] have been made to correct this effect.

Recombining the above equation with the first-order momentum equation (A16), summing over components, and using $\partial_t \Pi_{\alpha} = \partial_{1t}\Pi_{\alpha} + \partial_{2t}\Pi_{\alpha}$ gives a Navier-Stokes equation for an incompressible low Mach number flow:

$$\partial_t \Pi_{\alpha} + \partial_{\beta}\Pi_{\alpha\beta} = \sum_{\sigma} x^{\sigma}(\tau^{\sigma} - \tfrac{1}{2})\partial_{\beta}\partial_{\gamma}\Pi_{\alpha\beta\gamma} + \sum_{\sigma} F_{\alpha}^{\sigma}. \tag{A27}$$

Here, the mass fraction of component σ is written as x^{σ}. This can be expanded to give

$$\partial_t U_{\alpha} + U_{\beta}\partial_{\beta}U_{\alpha} + \frac{1}{\rho}\left[\partial_{\alpha}(c_s^2\rho) - \sum_{\sigma} F_{\alpha}^{\sigma}\right] = \nu\partial_{\beta}\partial_{\beta}U_{\alpha}. \tag{A28}$$

The kinematic viscosity ν is given by

$$\nu = c_s^2 \sum_{\sigma} x^{\sigma}(\tau^{\sigma} - \tfrac{1}{2}). \tag{A29}$$

The force term for immiscible fluids is usually treated by substituting the continuum approximation into Eq. (19).

It is perhaps worth noting that the force acting between components is (to second order in the expansion) proportional to the concentration gradient because of the lattice isotropy. It is possible that expansion beyond second order may provide a method for treating surfactant interactions as well [39].

[1] A. J. Bray, Adv. Phys. **43**, 357 (1994).
[2] H. Furukawa, Adv. Phys. **34**, 703 (1985).
[3] J. W. Cahn and J. E. Hilliard, J. Chem. Phys. **28**, 258 (1958).
[4] J. D. Gunton, M. S. Miguel, and P. S. Sahni, in *Phase Transitions and Critical Phenomena*, edited by C. Domb and J. Lebowitz (Academic, New York, 1983), Vol. 8, pp. 319–339.
[5] Y. Wu, F. J. Alexander, T. Lookman, and S. Chen, Phys. Rev. Lett. **74**, 3852 (1995).
[6] J. E. Farrell and O. T. Valls, Phys. Rev. B **40**, 7027 (1989).
[7] M. E. Cates, V. M. Kendon, P. Bladon, and J. C. Desplat, Faraday Discuss. **112**, 1 (1999).
[8] C. Roland and M. Grant, Phys. Rev. B **39**, 11 971 (1989).
[9] A. J. Wagner and J. M. Yeomans, Phys. Rev. Lett. **80**, 1429 (1998).
[10] R. B. Rybka, M. Cieplak, and D. Salin, Physica A **222**, 105 (1995).
[11] E. D. Siggia, Phys. Rev. A **20**, 595 (1979).
[12] M. San Miguel, M. Grant, and J. D. Gunton, Phys. Rev. A **31**, 1001 (1985).
[13] P. B. Sunil Kumar and M. Rao, Phys. Rev. Lett. **77**, 1067 (1996).
[14] E. Velasco and S. Toxvaerd, Phys. Rev. Lett. **71**, 388 (1993).
[15] K. E. Novik and P. V. Coveney, Phys. Rev. E **61**, 435 (2000).
[16] P. V. Coveney and K. E. Novik, Phys. Rev. E **54**, 5134 (1996).
[17] A. N. Emerton, P. V. Coveney, and B. M. Boghosian, Phys. Rev. E **56**, 1286 (1997).
[18] D. W. Grunau, T. Lookman, S. Y. Chen, and A. S. Lapedes, Phys. Rev. Lett. **71**, 4198 (1993).
[19] W. R. Osborn, E. Orlandini, M. R. Swift, J. M. Yeomans, and J. R. Banavar, Phys. Rev. Lett. **75**, 4031 (1995).
[20] H. Chen and A. Chakrabarti, Phys. Rev. E **55**, 5680 (1997).
[21] M. Grant and K. R. Elder, Phys. Rev. Lett. **82**, 14 (1999).
[22] S. Chen and T. Lookman, J. Stat. Phys. **81**, 223 (1995).
[23] F. J. Alexander, S. Chen, and D. W. Grunau, Phys. Rev. B **48**, 634 (1993).
[24] V. M. Kendon, J. C. Desplat, P. Bladon, and M. E. Cates, Phys. Rev. Lett. **83**, 576 (1999).
[25] D. H. Rothman and J. M. Keller, J. Stat. Phys. **52**, 1119 (1988).
[26] D. Grunau, S. Chen, and K. Eggert, Phys. Fluids A **5**, 2557 (1993).
[27] N. S. Martys and J. F. Douglas, Phys. Rev. E **63**, 031205 (2001).
[28] X. Shan and H. Chen, Phys. Rev. E **47**, 1815 (1993).
[29] S. Wolfram, J. Stat. Phys. **45**, 471 (1986).
[30] U. Frisch, B. Hasslacher, and Y. Pomeau, Phys. Rev. Lett. **56**, 1505 (1986).
[31] B. M. Boghosian, P. J. Love, and D. A. Meyer, Philos. Trans. R. Soc. London A **360**, 333 (2002).
[32] Y. H. Qian, D. d'Humiéres, and P. Lallemand, Europhys. Lett. **17**, 479 (1992).
[33] Y. H. Qian, Ph.D. thesis, École Normale Supérieure, Paris, 1990.
[34] X. Shan and H. Chen, Phys. Rev. E **49**, 2941 (1994).
[35] X. Shan and G. Doolen, J. Stat. Phys. **81**, 379 (1995).
[36] V. M. Kendon, M. E. Cates, I. Pagonabarraga, J. C. Desplat, and P. Bladon, J. Fluid Mech. **440**, 147 (2001).
[37] S. I. Jury, Ph.D. thesis, University of Edinburgh, 1999.
[38] H. Tanaka, Phys. Rev. Lett. **72**, 3690 (1994).
[39] H. Chen, B. M. Boghosian, P. V. Coveney, and M. Nekovee, Proc. R. Soc. London, Ser. A **456**, 2043 (2000).
[40] Y. H. Qian and S. A. Orszag, Europhys. Lett. **21**, 255 (1993).
[41] Y. H. Qian and Y. Zhou, Europhys. Lett. **42**, 359 (1998).